Multiple sensory neurons mediate starvation-dependent aversive navigation in *Caenorhabditis elegans*

Moon Sun Jang[a], Yu Toyoshima[a], Masahiro Tomioka[a], Hirofumi Kunitomo[a,1], and Yuichi Iino[a,1]

[a]Department of Biological Sciences, Graduate School of Science, The University of Tokyo, 113-0033 Tokyo, Japan

Edited by Paul W. Sternberg, California Institute of Technology, Pasadena, CA, and approved August 5, 2019 (received for review December 21, 2018)

Animals demonstrate flexible behaviors through associative learning based on their experiences. Deciphering the neural mechanisms for sensing and integrating multiple types of sensory information is critical for understanding such behavioral controls. The soil nematode *Caenorhabditis elegans* avoids salt concentrations it has previously experienced under starvation conditions. Here, we identify a pair of sensory neurons, the ASG neuron pair, which in cooperation with the ASER salt-sensing neuron generate starvation-dependent salt avoidance. Animals whose sensory input is restricted to only ASER failed to show learned avoidance due to inappropriately directed navigation behaviors. However, their navigation through a salt concentration gradient was improved by allowing sensory inputs to ASG in addition to ASER. Detailed behavioral analyses of these animals revealed that input from ASG neurons is required not only for controlling the frequency of initiating a set of sharp turns (called pirouettes) based on detected ambient salt concentrations but also adjusting the migration direction during pirouettes. Optogenetic activation of ASER by ChR2 induced turning behaviors in a salt concentration-dependent manner where presence of intact ASG was important for the starvation-dependent responses. Calcium imaging of the activity of ASG neurons in freely moving worms revealed that ASG is activated upon turning behavior. Our results indicate that ASG neurons cooperate with the ASER neuron to generate destination-directed reorientation in starvation-associated salt concentration avoidance.

associative learning | sensory processing | aversive navigation

Animals simultaneously detect various stimuli, such as chemical attractants and repellents that form spaciotemporal gradients, and physical stimuli such as temperature, light, and tactile stimuli and show flexible responses to them. Elucidating the mechanisms for the behavioral plasticity generated by integration of multiple sensory inputs is a central issue in neurobiology, but our understanding of such mechanisms remains limited. The soil nematode *Caenorhabditis elegans* responds by moving toward, or away from, various environmental cues (1) and shows a definite behavioral plasticity in gustatory, thermosensory, olfactory, and mechanosensory responses (2–5). The nervous system of the *C. elegans* hermaphrodite is composed of only 302 neurons and provides a platform for identifying complete neuronal processes from sensory inputs to behavioral outputs, because the cell identity and connections of all individual neurons have been completely characterized by reconstruction of electron microscope slices (6). Among 24 presumed ciliated amphid sensory neurons of the *C. elegans* hermaphrodite, the taste-sensing neurons called ASE play predominant roles in chemotaxis to NaCl and are involved in gustatory plasticity (7, 8). Behavioral responses to NaCl can be modulated by combinations of ambient NaCl concentration and food availability in *C. elegans*. For example, worms exposed to a low NaCl concentration along with food show an attraction toward low NaCl concentrations; however, this behavioral response to salt is converted into an aversion of a low-NaCl area after exposure to a low NaCl concentration without food, for example under starvation (7). We herein refer to the latter of these 2 scenarios (association of salt concentration and starvation) as taste avoidance learning. Our previous reports have shown that ASER, the right member of the bilateral ASE neuron pair, is essential for both food- and starvation-related salt chemotaxis plasticity and that the insulin signaling pathway in ASER is required for taste avoidance learning (7, 9–11).

Cooperation of functionally overlapping chemosensory neurons has been previously described in *C. elegans*. For example, multiple classes of sensory neurons, ASER, ASH, and ADF, all respond to salt stimuli and integration of their sensory input regulates behavioral responses to salt under certain conditions (12, 13). On the other hand, some sensory neurons show multimodal responsivity (14, 15) and their overlapping functions lead to the robustness and versatility of chemotactic behavioral responses (1).

Two behavioral strategies are known to be employed for salt chemotaxis in *C. elegans*: the pirouette strategy (a form of klinokinesis) and the weathervane strategy (a form of klinotaxis) (16, 17). During chemotaxis toward higher salt concentrations, pirouette strategy refers to a strategy in which worms exhibit increased frequency of "pirouettes" (a bout of reorienting turns) when they sense a decrease in ambient salt concentration. On the other hand, the weathervane strategy consists of curving toward the direction where higher salt concentration lies during their "run" (forward movement that is not a part of pirouette). Chemotaxis toward lower salt concentrations is achieved by the

Significance

Processing and integrating multiple sensory inputs are essential for generating appropriate behavioral output, where sensory information of food is particularly important. The soil nematode *Caenorhabditis elegans* remembers salt concentrations that they have experienced under starvation conditions and learn to avoid them by monitoring current salt concentrations with the salt-sensory neuron called ASER. Here, we described how a sensory neuron pair that was not previously implicated, called ASG, plays a pivotal role in driving food-related navigation; sensory input to these 2 sensory neurons is required for navigation to avoid salt concentrations associated with starvation. Our results show how integrated sensory information determines the bias of turning behaviors to efficiently navigate toward food in starved worms.

Author contributions: M.S.J., M.T., H.K., and Y.I. designed research; M.S.J. performed research; Y.T. and Y.I. contributed new reagents/analytic tools; M.S.J. and Y.I. analyzed data; and M.S.J., M.T., H.K., and Y.I. wrote the paper.

The authors declare no conflict of interest.

This article is a PNAS Direct Submission.

[1]To whom correspondence may be addressed. Email: kunitomo@bs.s.u-tokyo.ac.jp or iino@bs.s.u-tokyo.ac.jp.

This article contains supporting information online at www.pnas.org/lookup/suppl/doi:10.1073/pnas.1821716116/-/DCSupplemental.

Published online August 27, 2019.

reversal of the bias of turning frequency or curving direction. ASER is essential for both strategies: Ablation of ASER causes a defect in both the bias of pirouette and weathervane strategies. On the other hand, optogenetic activation of ASER has been shown to generate both behaviors (7, 18).

Here, we identified a pair of chemosensory neurons that are required, in addition to ASER, for taste avoidance learning and revealed the neuronal and behavioral mechanisms of this learning. We show that the starved worms with functional ASER and ASG neurons migrate away from the salt concentration which they have experienced under starvation conditions. Activity of ASG in cooperation with ASER regulates initiation of turning behavior to make them approach their preferred destination via the pirouette mechanism. ASG neurons are also important for proper regulation of turns during pirouettes. Our results show a way how input from multiple sensory neurons coordinates the bias of reorientation during pirouette and eventually generates the learned salt avoidance in starved animals.

Results

Sensory Inputs to ASER and ASG Neurons Are Required for Taste Avoidance Learning. Well-fed worms are attracted to the salt concentrations which they have experienced in the presence of food (henceforth called salt-attractive behavior for simplicity). In contrast, starved worms avoid the salt concentrations which they have experienced without food (called taste avoidance learning). For example, starved worms conditioned at 25 mM or 100 mM of NaCl tend to migrate to the highest or lowest salt concentration, respectively, when they are placed in the center of an assay plate with an NaCl gradient from ~35 to ~95 mM (Fig. 1*A*).

dyf-11 encodes a component of intraflagellar transport machinery, and mutants of *dyf-11* fail to perform salt chemotaxis due to the inability to form functional sensory cilia, although they show weak chemotaxis responses to volatile chemicals (13, 19). In previous reports, we used cell-specific rescue of the *dyf-11* mutants to demonstrate that chemosensory input to the ASER neuron alone was sufficient to drive salt-attractive behavior. However, it was not sufficient to drive taste avoidance learning (7, 11). To identify the sensory neurons involved in taste avoidance learning in addition to ASER, we constructed a series of cell-specific ciliated strains by using the *dyf-11*(*pe554*) mutant (*SI Appendix*, Table S2). As previously reported, worms expressing *dyf-11* solely in ASER by use of the *gcy-5* promoter failed to exhibit taste avoidance learning (Fig. 1*B* and *SI Appendix*, Fig. S1*A* and Table S2). By testing various cell-specific promoters to express *dyf-11*, we found that rescue of *dyf-11* in both the ASER and ASG sensory neurons recovered low-salt-avoidance behavior after conditioning at low salt concentrations under starvation conditions. The starved worms conditioned at high salt concentrations also appeared to be partially rescued for high-salt-avoidance behavior (Fig. 1*B* and *SI Appendix*, Figs. S1*A* and S2 and discussed below). In a complementary set of experiments, genetic ablation of ASG resulted in decrease of taste avoidance learning (Fig. 1*C*). To determine when the functions of ASG neurons are required for taste avoidance learning, we silenced ASG at particular time points using the histamine-gated chloride channel, HisCl1, under the ASG-specific *gcy-21* promoter (*SI Appendix*, Fig. S1*B*). Induced silencing of ASG by addition of 10 mM exogenous histamine during chemotaxis assays resulted in reduction of the learned chemotactic response only after conditioning without food, but not after conditioning with food (*SI Appendix*, Fig. S1*C*). Worms expressing the HisCl1 gene in multiple sensory neurons by the *tax-4* promoter showed reduced chemotaxis by addition of histamine, both after fed and starved conditioning (*SI Appendix*, Fig. S1*C*). These results combined

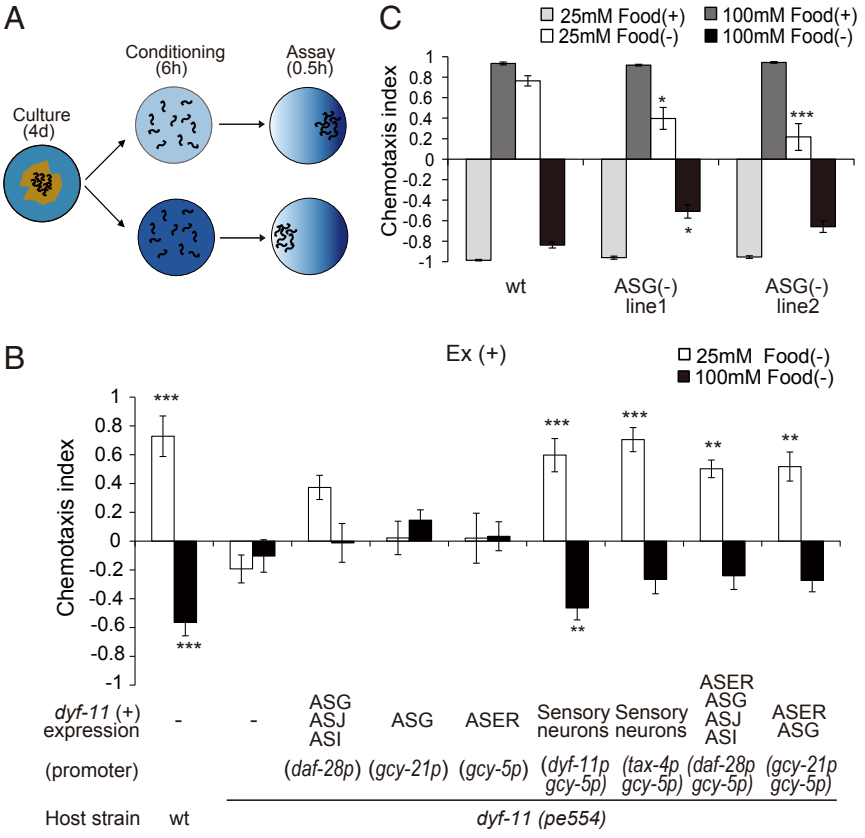

Fig. 1. Sensory inputs to ASER and ASG neurons are required for taste avoidance learning. (*A*) Procedure of taste avoidance learning assay used in this study and a representative result of wild-type (wt) animals. (*B*) Chemotaxis assay of *dyf-11*(*pe554*) and its cell-specific rescue strains. Cells that are rescued and promoters that are used to express functional *dyf-11* are shown below each pair of columns. Mean ± SEM; $n \geq 5$ assays; $^{**}P < 0.01$, $^{***}P < 0.001$ different from the ASER-ciliated strain, in which functional *dyf-11* gene is driven by the *gcy-5* promoter, conditioned at the same condition (ANOVA with Dunnett's posttest). (*C*) Chemotaxis indices of the ASG ablation strains that express mouse caspase1 in ASG neurons. Mean ± SEM; $n \geq 4$ assays; $^{*}P < 0.05$, $^{***}P < 0.001$ different from wt conditioned at the same condition (ANOVA with Dunnett's posttest).

suggest that the sensory inputs to ASG after conditioning under starvation may be required for taste avoidance learning.

ASG Modulates the Pirouette Mechanism after Starvation. Salt chemotaxis is known to be driven mainly by sensory input-dependent modulation of the occurrence of pirouettes (pirouette mechanism) and curving behaviors (weathervane mechanism) (7, 17). To investigate whether the ASG neurons regulate these behaviors during salt chemotaxis after starvation conditioning, we placed worms on a chemotaxis assay plate with an NaCl gradient from 35 to 95 mM for 10 min and analyzed each worm's behavior using a multiworm tracking system (7, 20). When the wild-type animals were conditioned at 25 mM of NaCl without food they showed higher pirouette frequency during perceived decrease in salt concentration (dC/dL < 0), whereas they showed lower pirouette frequency during perceived increase in salt concentration (dC/dL > 0); namely, they utilized the pirouette mechanism, or klinokinesis (Fig. 2*A* and *SI Appendix*, Fig. S2*A*). When they were conditioned at 100 mM of NaCl without food, these behavioral biases were reversed (Fig. 2*A* and *SI Appendix*, Fig. S2*E*). On the other hand, the stable transgenic strain in which *dyf-11* was rescued only in ASER (hence it is expected that only ASER can sense chemicals; hereafter called the ASER-ciliated strain) showed strong defects in the bias of pirouette frequency after conditioning at either 25 mM or 100 mM (Fig. 2*A* and *SI Appendix*, Figs. S2 *A*, *B*, *E*, and *F*). The behavioral defect was rescued by the expression of *dyf-11* under the *gcy-21* promoter, which drove expression in ASG in the ASER-ciliated strain after 25 mM conditioning (Fig. 2*A* and *SI Appendix*, Fig. S2*B*). The sensory input to ASG does not seem to contribute much to the weathervane mechanism after salt conditioning without food (Fig. 2*B* and *SI Appendix*, Figs. S2 *C*, *D*, *G* and *H*). On the other hand, the ASER- and ASG-ciliated worms conditioned at 100 mM of salt under starvation showed tendencies to slightly recover the pirouette and the weathervane mechanisms compared to the ASER-ciliated worms but did not show substantial recovery (Fig. 2 and *SI Appendix*, Fig. S2 *E–H*). These results suggest that ASG contributes to increased frequency of pirouette upon decrease of salt concentration (dC/dL < 0) when worms were conditioned at 25 mM of NaCl without food. The weak or nonsignificant recovery in the ASER- and ASG-ciliated worms after conditioning at 100 mM is consistent with the marginal but nonsignificant recovery of overall high-salt avoidance and the weak defect of high-salt avoidance in ASG-ablated worms (Fig. 1 *B* and *C*). It is likely that an unknown neuron(s) is required in addition to ASER and ASG for high-salt avoidance.

Activation of ASER and ASG Promotes Turning Behavior in a Conditioning-Dependent Manner. Previously, we demonstrated that activation of ASER using Channelrhodopsin-2 (ChR2) either promoted or suppressed turning behaviors depending on the salt concentration of conditioning with food (7). To examine the effects of ASER activation on turning behavior after salt conditioning without food, ChR2 was expressed in ASER neurons in the mutant background of *lite-1* which encodes an intrinsic photoreceptor (to eliminate irrelevant behavioral response to the light-emitting diode light source) and examined behavioral changes upon illumination with blue light. Activation of ASER promoted turning events in worms starved at 25 mM (Fig. 3 *G*, top graph and Fig. 3*I*). Since ASER is activated upon decrease in salt concentration, these behavioral changes after starvation conditioning could contribute to avoidance of low salt concentrations (*SI Appendix*, Fig. S3*A*). On the other hand, stimulation of ASER seemed to suppress turning immediately after illumination when worms were conditioned at 25 mM of NaCl with food and were transferred to an assay plate containing 50 mM NaCl (Fig. 3 *A*, top graph and Fig. 3*C*), but there was no significant difference between pre- and postillumination or *all-trans* retinal-positive (ATR+) and ATR− conditions These behavioral changes were reversed after conditioning at 100 mM NaCl (Fig. 3 *B* and *H*, top graphs and Fig. 3 *D* and *J*). The ASER-ciliated worms showed significant defects in their responses after starvation; ASER activation induced turning behavior after starvation conditioning at 100 mM NaCl (Fig. 3*H*, second graph and Fig. 3*J*), while responses after 25 mM conditioning as seen in wild-type animals were not observed (Fig. 3*G*, second graph and Fig. 3*I*). On the other hand, rescue of ASG sensory input in the ASER-ciliated background in a strain called JN2129 resulted in partial recovery of turning events, resulting in a behavioral profile similar to wild-type animals conditioned at 25 mM or 100 mM NaCl without food (Fig. 3 *G* and *H*, third graphs and Fig. 3 *I* and *J*). Moreover, we examined behavioral changes when ASER was activated in *dyf-11*(+) worms in which ASG was ablated by expression of mouse caspase1. The ASG-ablation worms showed defective responses to ASER activation after starvation conditioning: They showed a decrease in turning events compared with wild-type animals when conditioned at 25 mM salt and aberrant increase in turning events when conditioned at 100 mM salt without food (Fig. 3 *G* and *H*, bottom graphs and Fig. 3 *I* and *J*). These phenotypes were similar to those seen in ASER-ciliated worms. Without ATR, which is necessary for the light response of ChR2 activity, turning event rate was not affected by light illumination in any of the strains we tested (Fig. 3 *E*, *F*, *K*, and *L*). We also confirmed that expression of ChR2 in ASER in the *lite-1* mutant background does not affect taste

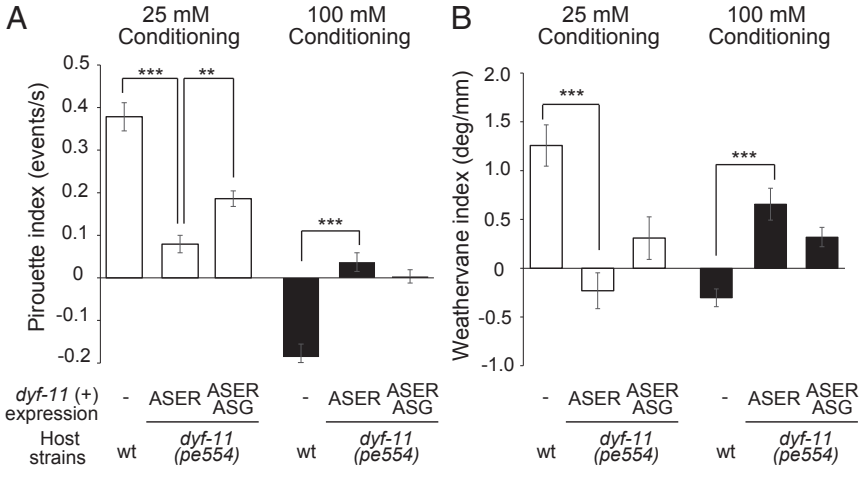

Fig. 2. Turning bias in pirouette mechanism is modulated by sensory input to ASG. Bias of pirouette mechanism (*A*) and weathervane mechanism (*B*) represented by the pirouette index and the weathervane index, respectively. Positive indices indicate migration bias toward higher salt concentrations and negative indices indicate migration bias toward lower concentrations. Results of wild type (wt), ASER-ciliated strain, and both ASER- and ASG-ciliated strain conditioned at 25 mM or 100 mM NaCl without food. Mean ± SEM; $n \geq 16$ assays; $^{**}P < 0.01$, $^{***}P < 0.001$ different from wild type or *dyf-11* background mutants conditioned at the same condition (ANOVA with Dunnett's posttest).

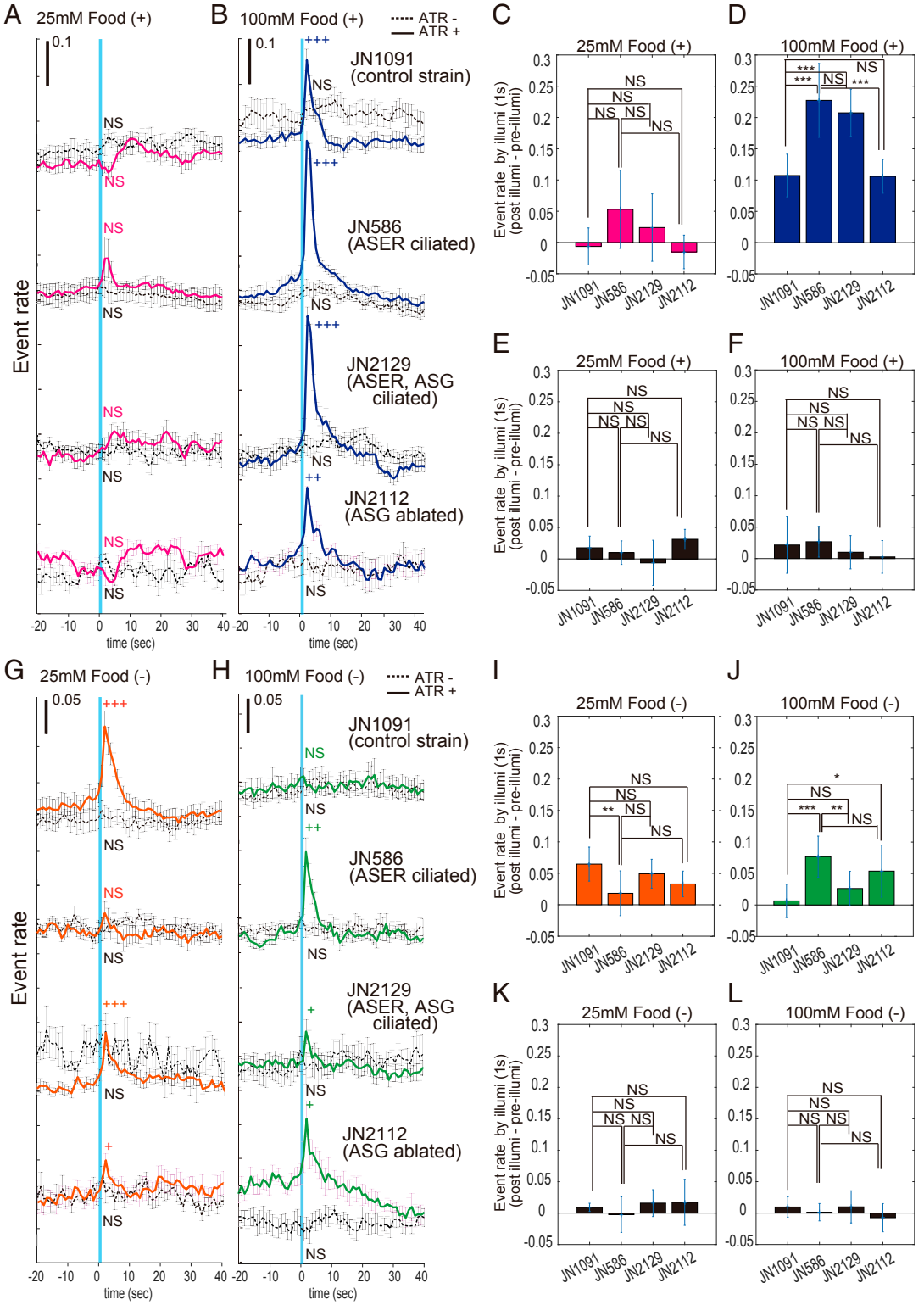

Fig. 3. Input to ASG modulates ASER-evoked turning behavior under starved conditions. (*A*, *B*, *G*, and *H*) The turning/reversal/pausing rate evoked by optical stimulation of ASER by ChR2 (blue stripe at time 0). Worms were conditioned at 25 mM or 100 mM NaCl with food or without food and illuminated with blue light on agar plates containing 50 mM NaCl. Error bars and shaded regions represent SEM. (*C–F* and *I–L*) The colored bar graphs show the change in rate of turning events by photostimulation. The averaged turning event in a 10-s window before stimulation was set as the preillumination period, and the averaged turning events in a 3-s window after stimulation was set as the postillumination period. Cultivation conditions are listed at the top of each bar graph. (*E*, *F*, *K*, and *L*) The black bars represent trials where ATR was not added as a negative control. Mean ± SEM; $n \geq 6$ assays; NS, not significant; $^{+}P < 0.05$, $^{++}P < 0.01$, $^{+++}P < 0.001$ difference between pre- and postillumination; (paired *t* test); $^{*}P < 0.05$, $^{**}P < 0.01$, $^{***}P < 0.001$ difference from JN1091 or JN586 (Tukey's multiple comparison test).

avoidance learning (*SI Appendix*, Fig. S3*B*). These results indicate that presence of the ASG neuron pair is important for starvation-dependent behavioral changes upon activation of ASER which correspond to the pirouette mechanism.

ASG Neurons Show Spontaneous Activity but Do Not Respond to Salt Stimuli. We then examined whether activity of ASG neurons is altered by exposure to salt or to starvation. We have previously demonstrated that ASER is activated by a decrease in detected salt concentration, for example from 50 to 25 mM, and the magnitude of the activation varied depending on conditioned salt concentrations when measured with the calcium indicator GCaMP (7). We simultaneously monitored the calcium levels of multiple sensory neurons using the calcium indicator YC2.60 localized to the nucleus after stepwise decrease in salt concentration. We compared the responses of each sensory neuron upon salt concentration decrease from 50 to 25 mM in worms conditioned with or without food. Our results showed that there was no difference in the ASER responses between fed and starved worms (Fig. 4*A* and *SI Appendix*, Fig. S4*A*). On the other hand, ASGR and ASGL neurons did not show any clear response to the salt stimulation (Fig. 4 *B* and *C* and *SI Appendix*, Fig. S4 *B* and *C*). We next examined ASER and ASG responses to various intensities of salt stimuli, namely step changes of 1, 5, and 25 mM from 50 mM of NaCl. While ASER was always activated upon decrease in salt concentration, ASG neurons did not show detectable activity changes in response to any salt stimulus intensity (*SI Appendix*, Fig. S4*D*). The amplitude of calcium transients was smaller in the nucleus than in the cytoplasm in ASER, presumably because changes in calcium levels in the nucleus by salt stimulation were derived from those in the cytoplasm. To test the possibility that calcium responses of ASG are more prominent in cytoplasm, we examined animals in which YC2.60 or GCaMP6s, another calcium probe with high sensitivity, was expressed in the ASG cell body after worms were conditioned at 25, 50, or 100 mM of NaCl. Again, ASG neurons did not show discernible response to salt stimulus (*SI Appendix*, Figs. S4 *E*, *F*, and *I*). Unexpectedly, however, we found they showed spontaneous activity independent of salt stimulus (*SI Appendix*, Fig. S4 *E* and *F*). We quantified these responses using a peak fitting algorithm called constrained deconvolution (21). Both the frequency and average size of ASGR activity peaks after 25 mM salt conditioning and the average size of ASGR activity peaks after 50 mM salt conditioning under starvation were significantly higher when compared with those under feeding (Fig. 4*D* and *SI Appendix*, Fig. S4*G*). On the other hand, the amplitudes of activity peaks of ASG neurons were significantly lower in the *dyf-11* mutant compared with wild-type animals when conditioned at 50 mM salt without food (Fig. 4*D*), suggesting that spontaneous ASG activity caused by starvation is dependent on cilium function. The basal calcium levels were not

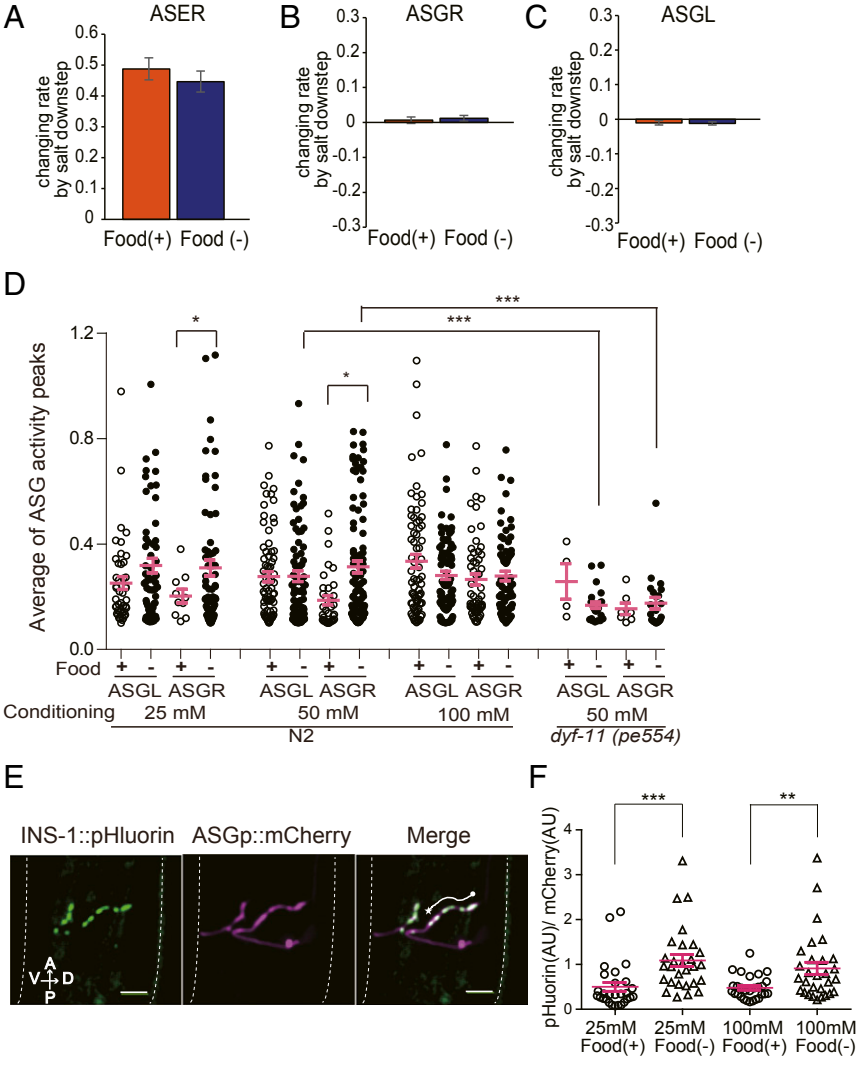

Fig. 4. Calcium responses of the ASER and ASG neurons in food(+/–) conditioned worms. (*A*–*C*) Averages of the fluorescence changes during the 25 s before and after the salt stimulus in the nucleus of ASER (*A*), ASGR (*B*), or ASGL (*C*). Worms were conditioned at 50 mM NaCl with food or without food for at least 6 h. $n \geq 3$ mean ± SEM. (*D*) Averaged size of ASG activity peaks in the cell body of ASGR and ASGL expressing the calcium probe YC2.60 in the wild-type N2 conditioned at 25, 50, or 100 mM salt with or without food. The *dyf-11* mutant was conditioned at 50 mM salt with or without food. Statistics for ASG responses are $^{*}P < 0.05$, $^{***}P < 0.001$ (2-tailed *t* test with Bonferroni correction). (*E*) Maximum intensity projection images of the wild type expressing both INS-1::pHluorin and mCherry in ASG. The fluorescence intensities of INS-1::pHluorin and mCherry were measured along the 15-μm white line which extends from the position indicated by the star to the tip (circle) of the axon. (Scale bars, 10 μm.) (*F*) Quantified fluorescence intensity ratios of INS-1::pHluorin to mCherry. Animals were conditioned at 25 or 100 mM salt with (○) or without (△) food. $n \geq 28$; $^{**}P < 0.01$, $^{***}P < 0.001$ different from fed or starved conditioning at the same salt concentration (2-tailed Welch's *t* test). Bars represent mean ± SEM.

different between conditioning groups (*SI Appendix*, Fig. S4*H*). In addition, we investigated the possibility of increased release of neuromodulators, such as neuropeptides, in ASG under starvation by monitoring release of an insulin-like peptide, INS-1, fused with pHluorin, a pH-sensitive derivative of green fluorescent protein (22). It was reported that INS-1 was packaged into dense core vesicles (DCVs) along with other neuropeptides and localized to the axons of several neurons (9, 23) and that DCV release was monitored by pHluorin-fused neuropeptides (24). The INS-1::pHluorin fluorescence in the ASG axon was significantly higher after starvation conditioning with 25 or 100 mM salt than that after fed conditioning, suggesting that neuropeptidergic signaling from ASG is up-regulated after starvation conditioning. (Fig. 4 *E* and *F*). Collectively, these results imply that activities of ASG neurons and neurotransmission from ASG are higher after starvation compared to those after fed conditioning.

ASG Neurons Are Activated during Turning Behaviors. To examine whether ASG activity is related to any specific behavior, we simultaneously monitored the activity of ASG neurons (with GCaMP6s) and the behaviors of freely moving worms under both fed and starved conditions after previous feeding or food deprivation. These tests were performed on plates without a salt gradient. Worms showed occasional spontaneous turning, which was initiated by reversal and followed by a sharp turn, in which the worm bends its whole body and assumes an omega-like shape followed by resumption of forward locomotion. The ASG neurons were gradually activated during a reversal movement followed by turning behavior, and the activation lasted for several minutes after the turn (Fig. 5 *A* and *B*). We quantified the activity during each part of the behavioral sequence: prereversal, during reversal, and postreversal. The ASG activity was significantly increased over the switch from reversal to postreversal, and this tendency was conserved across all feeding conditions (Fig. 5*C* and *SI Appendix*, Fig. S5*A*). These results suggest that the activity of ASG may be related to and modulate behaviors during or after turning. No activity change of this neuron was observed upon touching a food patch (*SI Appendix*, Fig. S5*B*).

ASG Contributes to Determining the Direction of Turning during Pirouettes after Starvation. Activation of ASG neurons during and after reversal/sharp turns prompted us to investigate whether ASG has any roles after initiation of pirouettes. To do so, we performed detailed analyses of the chemotaxis behavior on a salt gradient from 35 to 95 mM using the multiworm tracker. The ASER- and ASG-ciliated strain conditioned at 25 mM or 100 mM of salt under starvation conditions moved toward high or low salt concentrations, respectively, like the wild type, although the tendency was weaker for 100 mM-conditioned animals (*SI Appendix*, Fig. S6 *A* and *B*). However, the ASER-ciliated strain did not move in a biased manner, and their chemotaxis index showed almost zero values (*SI Appendix*, Fig. S6 *A* and *B*). We then analyzed the turning angles in each pirouette turn. As mentioned earlier, the term "pirouette" has been defined as bouts of sharp turns (change of centroid movement direction by more than 280°) separated by time spans shorter than T_{crit} (3.18 s), based on the previous analyses (17). In most cases the first turn corresponds to a switch from forward to backward locomotion (reversal). Bearing (B) is defined as the angle of the salt gradient vector (direction of the steepest positive slope) relative to the direction of the animal's locomotion (*SI Appendix*, Fig. S6*C*) (16, 17). Therefore, when the absolute value of bearing is small, the worm is moving in the direction toward the salt peak and when the bearing is around ±180° the worm is moving away from the peak. We first compared bearing before the first reversal (to be exact, the first sharp turn, but for the sake of simplicity we refer to it as reversal) to bearing after pirouette (*SI Appendix*, Fig. S6*C*). In wild-type animals conditioned at 25 mM, bearing before reversal was enriched around ±120° (Fig. 6*A*), consistent with the more frequent initiation of pirouette during decrease of salt concentration (pirouette mechanism). On the other hand, B_{after} (bearing after pirouette) was enriched around zero, namely orientating toward the salt peak, which was expected, because the worms were starved at a low salt concentration. The difference between the angles B_{before} and B_{after} (ΔB), which corresponded to the angle of reorientation, fell most frequently around ±180° (Fig. 6*A*), suggesting that once a pirouette is initiated worms tend to eventually turn to the opposite direction. However, the choice of turning angle turned out not to be random. When we added B_{before} and ΔB after shuffling them but maintaining the distribution of each, distribution of the resulting value, $B^{indep}{}_{after}$, showed a much smaller bias than the actual distribution of B_{after} (Fig. 6*A*). These results strongly suggested that the angle of reorientation is determined depending on B_{before} so that the worm is oriented toward the peak after the pirouette. Similarly, in wild-type animals conditioned at 100 mM, B_{after} was enriched around ±180°, namely orienting away from the peak (Fig. 6*D*). ΔB was most frequently around ±180°, but the orientation angle was not randomly chosen from this distribution but was chosen so that the worm was oriented away from the peak after the pirouette (Fig. 6*D*). On the other hand, B_{after} in the ASER-ciliated strain showed a weak tendency of enrichment around ±180°after conditioning at 25 mM, and around 0°after conditioning at 100 mM, which are opposite to wild type (Fig. 6 *B* and *E*). These defects were reversed by the cilia formation of ASG, although again the recovery was weak after conditioning at 100 mM (Fig. 6 *C* and *F*).

We further investigated how the direction of movement changed after the first reversal in each pirouette. Pirouettes were classified to bins of initial bearing, and the average value of bearing in each class gradually approached zero with the passage of time in the wild-type or the ASER- plus ASG-ciliated strains after conditioning at 25 mM of salt under starvation conditions (Fig. 7 *A* and *C*, *Upper*). Conversely, the average value of bearing in each class gradually shifted away from zero with the passage of time in the wild-type or the ASER- plus ASG-ciliated strains after conditioning at 100 mM of salt under starvation conditions (Fig. 7 *D* and *F*, *Upper*). On the other hand, the ASER-ciliated strain did not show such reorientation, with a possible tendency toward the opposite direction (Fig. 7 *B* and *E*, *Upper*). Although the shift of locomotion direction toward or away from a salt concentration peak is phenomenologically similar to the weathervane mechanism and is considered a form of klinotaxis, the speed of the shift that occurs during pirouette was much faster than that during a run, which is, by definition, when the weathervane mechanism occurs (Fig. 7, *Lower*). Therefore, we call this biased turning a "directed pirouette." To further characterize this behavior, we classified pirouettes to bins of bearing just after the first reversal, aligned them at the position of first reversal, and plotted average positions of worms at each time point thereafter. On average, wild-type animals conditioned at 25 mM of salt under starvation turned toward the salt peak after the first reversal and the worms conditioned at 100 mM of salt under starvation turned away from the salt peak after the first reversal (Fig. 8 *A*, *Left*), irrespective of initial orientation. The ASER-ciliated strain showed biased turning after the initial reversal in the wrong direction after conditioning at 25 mM (Fig. 8 *A*, *Upper Middle*). The aberrant bias of reorientation in the ASER-ciliated strain appeared to be rescued by restoration of sensory input to ASG (Fig. 8 *A*, *Upper Right*).

To investigate which behavioral elements contribute to directed pirouettes in the wild type, we quantified averaged change in the direction vector caused by each behavioral element, forward, backward, reversal, omega, deep turn, and so on. Only the component of the averaged vector in the rotational direction was accessed. The contributions of reversal (sharp turn without assuming an omega shape) and omega (any event involving rounding

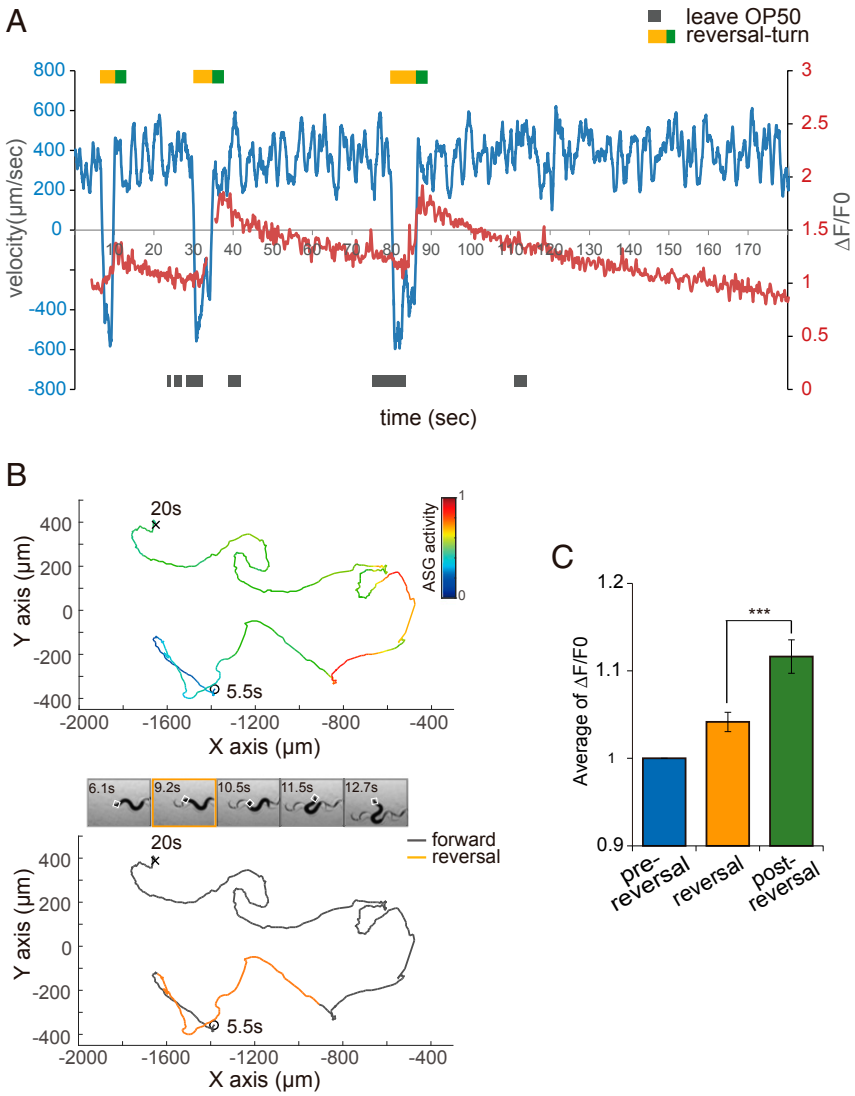

Fig. 5. ASG is activated during turning behavior. (*A*) Representative result of tracking imaging of a fed worm on NGM with *E. coli* OP50. Blue and red lines represent moving speed of the worm and activity of ASG neurons, respectively. Negative velocity values mean the worm was moving backward. Gray boxes represent the times at which the worm moved out of *E. coli* OP50 covered area. Orange-green box represents the section at which the worm showed behavioral change phase from reversal to turning. (*B*) A representative trace of activity of ASG neurons and worm's locomotion during 5.5-s to 20-s time points in A. The lines indicate the trajectory of worm's head position. Activity (*Top*) and reversal behavior (*Bottom*) are shown in color. The reversal behaviors occurred between 6.9 s and 9.7 s in A (orange, *Bottom*). (*C*) Quantification of ASG activity according to behavioral changes. Averages of the ASG activity for each phase of locomotion, before reversal, during reversal, and after reversal, normalized to pre-reversal. Statistics for ASG activity are $***P < 0.0001$; $n = 26$ compared with reversal locomotion (Tukey's multiple comparison test). Bars represent mean ± SEM.

up of the worm's posture) were the highest in the wild type after conditioning at 25 or 100 mM of salt under the starvation condition (*SI Appendix*, Fig. S7). Therefore, we tentatively conclude that directional pirouette is mainly achieved by repetitive sharp turns that occur when the worm moves toward an inappropriate direction. All results considered, ASG is important for determining the turning direction during pirouettes (directed pirouettes) in worms conditioned by starvation, especially at a low salt concentration.

Discussion

Although sensory neurons make up only a small fraction of the entire nervous system, they play important roles in behavioral plasticity in *C. elegans*. The sensory neurons have overlapping roles in sensing various environmental stimuli and regulating behavioral output (1, 13, 15, 25). Worms are attracted to food odor such as diacetyl while they avoid toxic chemicals or hyperosmotic concentrations of water-soluble chemicals (12, 26–28). Exposure to unfavorable but not immediately threatening conditions such as hunger leads to slow changes of the internal states in animals and induces behavioral changes so that they can escape these unfavorable conditions. To date, several studies have described how conditions related to food lead to behavioral changes through sensory perception in *C. elegans* (25, 29–31).

Here, we aimed to identify specific sensory neurons required for taste avoidance learning that comprised a major salt-sensing neuron, ASER, and previously unknown sensory neurons. The basis of this search was that data showed the sensory input to ASER alone was sufficient for the salt attraction behavior after being fed in the presence of salt but was insufficient for avoidance of the salt concentrations experienced during starvation. The change of salt concentration is sensed by the ciliated sensory endings of ASER, whose absence results in defective salt chemotaxis (7, 11). Our cell-specific rescue experiments using the *dyf-11* gene suggested that sensory inputs to both ASER and ASG are required for the taste avoidance behavior. The sensory inputs to ASH, known as polymodal nociceptive sensory neurons, were not involved in taste avoidance learning (*SI Appendix*, Table S2; the worms expressing *dyf-11* in both ASER and ASH by the *gcy-5* and *sra-6* promoter). In our observations, we found that although ASG shows no responses to salt concentration changes, consistent with a previous study (13), its activation was correlated with reversals and subsequent turns (Fig. 5). It has been described that several sensory neurons affect the probability of reversals and turns in a manner related to food conditions. In particular, laser ablation of ASG caused decreased frequency of longer reversals and omega turns, but not short reversals, compared to that of untreated animals after a long food-free exploration time (25). Frequency of pirouette

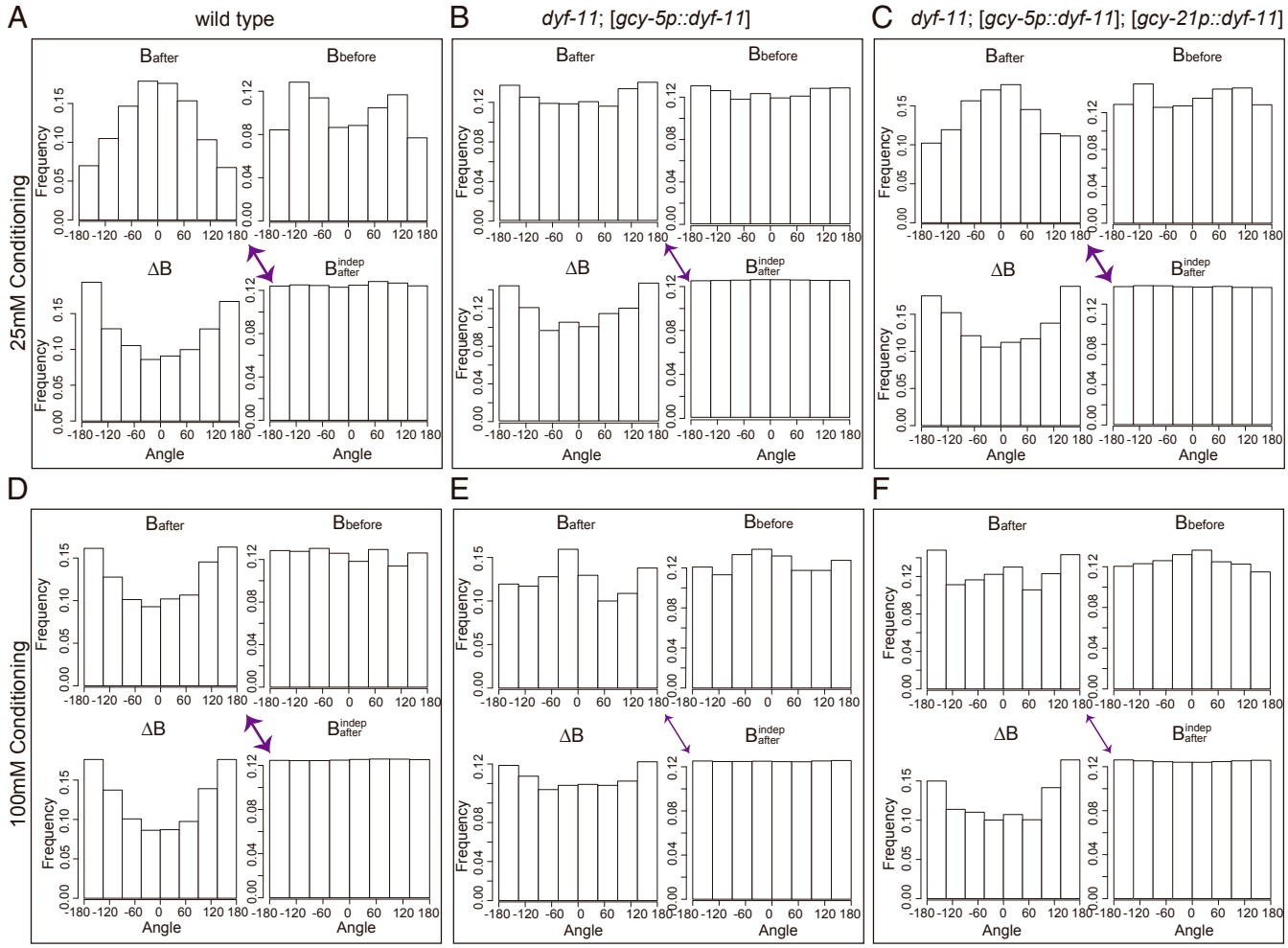

Fig. 6. Analysis of bearing distributions during salt chemotaxis. Histograms of bearing before the first reversal in pirouette (B_{before}), bearing after pirouette (B_{after}), changes in bearing ($\Delta B = B_{after} - B_{before}$), and reconstruction of bearing after pirouette based on distributions of B_{before} and ΔB ($B^{indep}{}_{after}$) are indicated for wild type (*A* and *D*), ASER-ciliated strain (*B* and *E*), and both ASER- and ASG-ciliated strain (*C* and *F*). Worms were conditioned at 25 mM (*A*–*C*) or 100 mM (*D*–*F*) salt without food. The arrows indicate the significance level of difference between distribution of B_{after} and $B^{indep}{}_{after}$, which corresponds to the contribution of the directed pirouette mechanism. The thick, medium, and thin arrows indicate $P < 2.23e\text{-}16$, $P = 8.396e\text{-}07$, and $P < 0.01$, respectively (Mardia–Watson–Wheeler test). Difference in the distribution of B_{after} between 2 strains under the same conditioning were significant; $P < 2.2e\text{-}16$ (N2 vs. ASER-ciliated strain), $P < 2.2e\text{-}16$ (ASER-ciliated strain vs. ASER- and ASG-ciliated strain), $P < 2.444e\text{-}06$ (N2 vs. ASER- and ASG-ciliated strain) under 25 mM conditioning, $P < 2.2e\text{-}16$ (N2 vs. ASER-ciliated strain), $P < 0.00012$ (ASER-ciliated strain vs. ASER- and ASG-ciliated strain), and $P < 5.503e\text{-}08$ (N2 vs. ASER- and ASG-ciliated strain) under 100 mM conditioning (Mardia–Watson–Wheeler test).

behavior was increased when worms conditioned at a low salt concentration migrated toward a low salt concentration (*SI Appendix*, Fig. S2 *A* and *B*). These enhanced behavioral responses might be due to starvation-induced activity of ASG. In fact, the amplitudes of calcium peaks and release of a neuropeptide in ASG were increased by starved conditioning compared to fed conditioning (Fig. 4 *D* and *F*). There was no apparent rule in the timing and rate of the activation of ASG, but change in the size of stochastic activity might be a manifestation of altered intrinsic neuronal properties caused by starvation. The higher neuronal activities of ASG after starvation require the intact cilia (Fig. 4*D*), consistent with the finding that the cilium function of ASG is required for low-salt avoidance after starvation conditioning (Fig. 1*B*). On the other hand, the contribution of ASG to high-salt avoidance is small compared to that to low-salt avoidance after starvation conditioning. The ASER- and ASG-ciliated strain did not fully rescue but showed a weak tendency to rescue high-salt avoidance in several behavioral analyses (Figs. 1*B*, 2, 7*F*, and 8*A* and *SI Appendix*, S6 *A* and *B*). These results suggested that the cooperative functions of unidentified sensory neuron(s) along with ASER and ASG are required for salt avoidance learning after high-salt conditioning under starvation.

It is currently unknown how output from ASG regulates the behavioral response to NaCl after starvation, but a hypothetical possibility is that activated ASG regulates the signal transmission between ASER and its immediate downstream interneurons, AIA, AIY, and AIB. In fact, based on recent electron microscopy analysis (https://wormwiring.org/), these downstream interneurons also have incoming chemical synapses or electrical connections with ASG. Our previous reports have described that the synaptic plasticity between ASER and interneurons led to behavioral changes such as the pirouettes and weathervane mechanism depending on a previously experienced salt concentration in the conditioning with food (7, 18). Our current study shows that ASER responses upon salt stimuli did not substantially change dependent on starvation conditioning (Fig. 4*A* and *SI Appendix*, Fig. S4*A*), whereas behavioral responses upon ASER activation dramatically changed after starvation conditioning, and sensory inputs to ASG are required for this behavioral change (Fig. 3). These findings suggest that functioning of the neural circuit

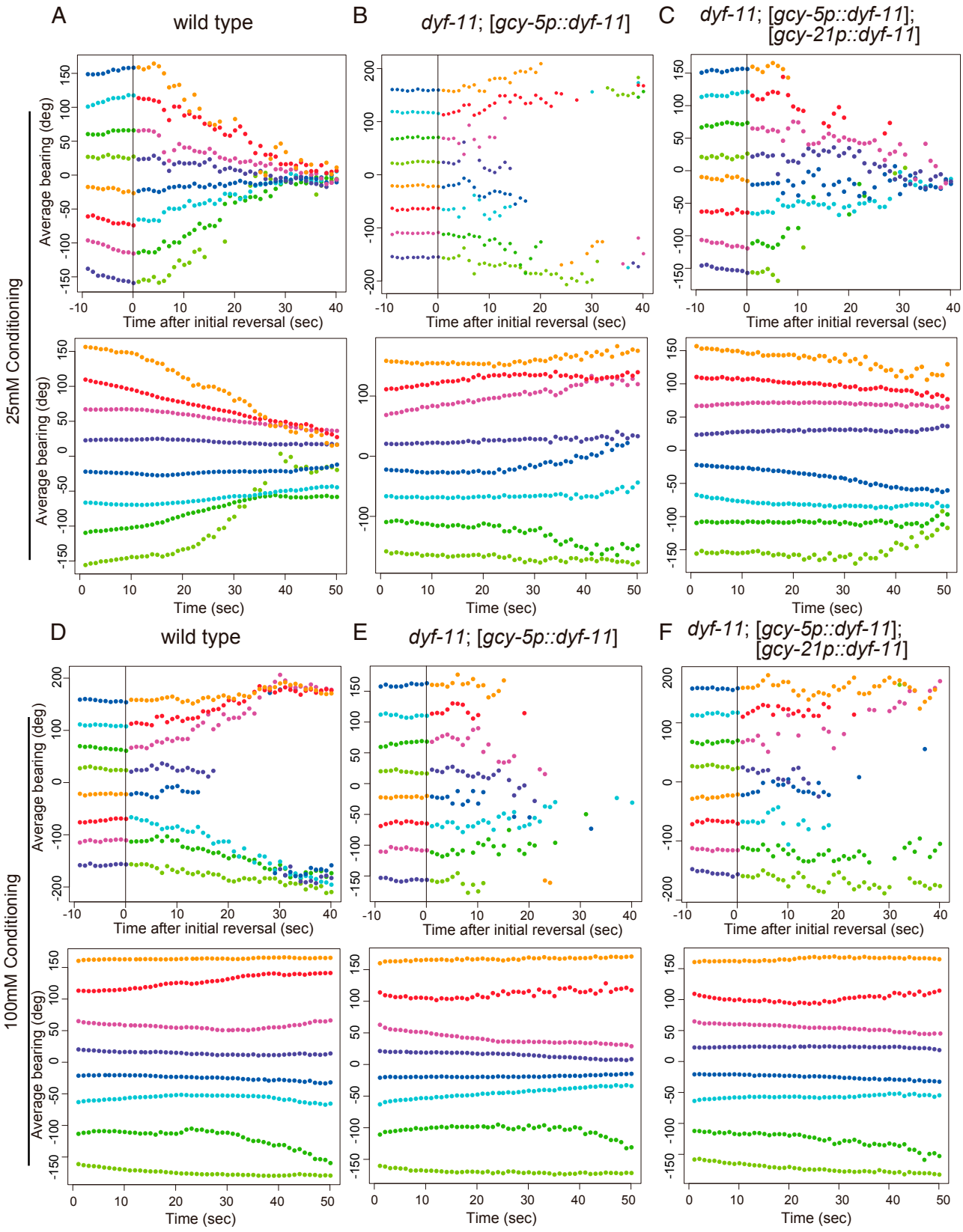

Fig. 7. ASG contributes to switching the navigation direction relative to salt gradient. (*A–F*, *Upper*) The change of averaged bearing for a period of 10 s before and 40 s after the initial reversal of pirouette. Pirouette events were classified in 45° bearing bins after initial reversal, and bearing thereafter was circularly averaged for each class. When the distribution of the angles was not statistically different from random distribution as assessed by the Rayeigh test at $\alpha = 0.1$, the value was not plotted. (*A–F*, *Lower*) The change of averaged bearing during runs (migration tracks excluding pirouettes). Worm tracks were classified in 45° bearing bins at each time point during run and subsequent bearing was circularly averaged as above. Worms were conditioned at 25 mM (*A–C*) or 100 mM (*D–F*) salt without food.

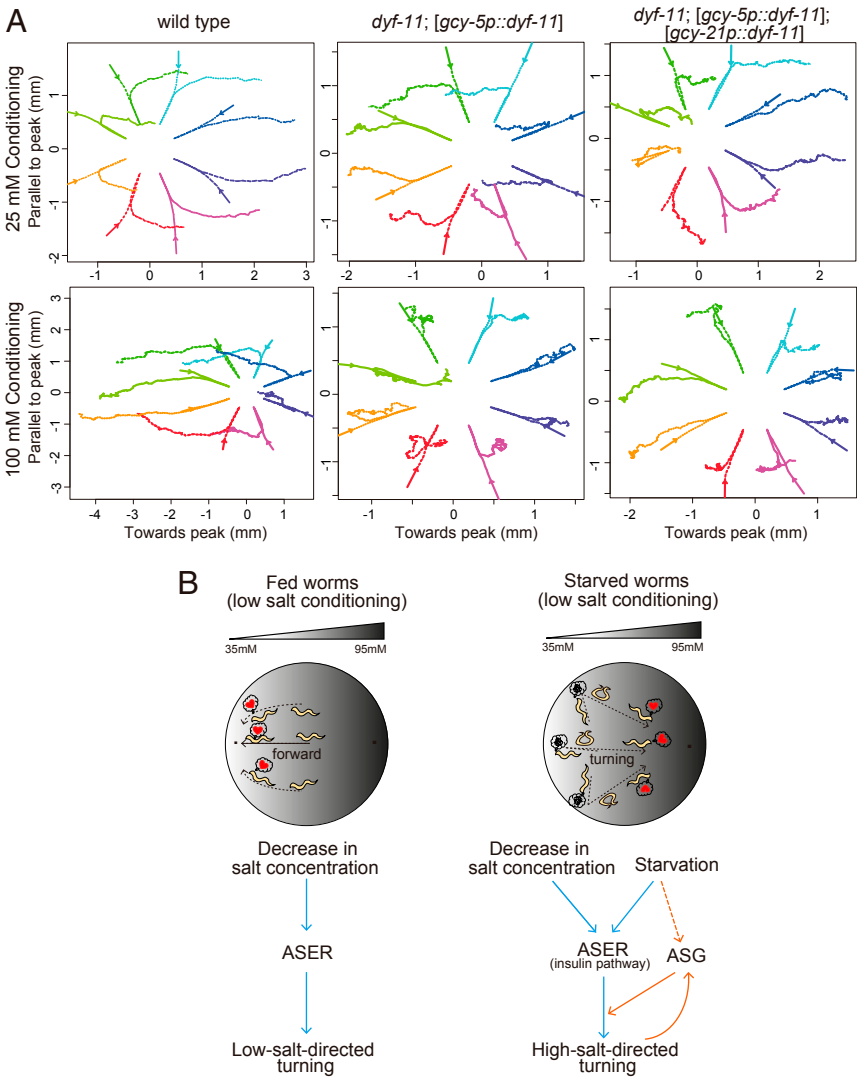

Fig. 8. ASG contributes to directed pirouette. (*A*) Tracks of worms during and after pirouette. Pirouettes were classified in 45° bearing bins right after the first reversal and the tracks were aligned at the position where worms switched from forward locomotion to reversal. The positions thereafter for 100 s were averaged and plotted for each class. Tracks were rotated so that salt gradient at the first reversal is to the right side, and for presentation purposes the initial position was separated for each class. All worms used in this analysis were conditioned at the 25 mM (*Upper*) or 100 mM (*Lower*) salt without food: wild type (*Left*), ASER-ciliated strain (*Middle*), and both ASER- and ASG-ciliated strain (*Right*). (*B*) Schematic model representing taste navigation circuits after learning of food conditions. When fed worms conditioned at a low salt concentration move toward low salt concentration, they show forward movement and curve toward a lower salt concentration. These behaviors are mediated by activation of ASER upon decrease in salt concentration (*Left*). When starved worms conditioned at a low salt concentration move toward low salt concentration, they show turning behavior and avoid low salt concentration. This behavior is also mediated by activation of ASER, but in this case under the control of ASG neurons. Further activation of ASG neurons generates the optimum turning behavior depending on a current direction of worm trajectory (*Right*).

downstream of ASER is altered dependent on starvation conditioning and ASG functions, the detailed mechanisms of which should be further explored.

Based on our results, we propose the following model (Fig. 8*B*). Fed worms conditioned at a low salt concentration with food show attraction toward lower salt concentrations. Under these conditions, activation of ASER upon detected decrease in salt concentration promotes (or does not prevent) forward locomotion (7) (Fig. 8 *B*, *Left*). On the contrary, starved worms conditioned at a low salt concentration without food show the avoidance of lower salt concentrations. Under these conditions, activation of ASER upon detected decrease in salt concentration ($dC/dt < 0$) promotes turning, and the activity of ASG is essential for this control. Previous studies suggested that insulin-like signaling mediates starvation signals by acting in ASER and regulating its synaptic output (7, 9–11, 32). In addition, increased basal activity and neuromodulator release of ASG upon starvation may also contribute to directing low-salt avoidance, for example by making neurons downstream of ASER, such as interneurons that direct turning, to be more sensitive to ASER input (Fig. 8 *B*, *Right*). Interestingly, ASG is required for suppression of increased turning frequency upon ASER activation after high-salt conditioning (Fig. 3*H*), suggesting that ASG can modulate both promotion and suppression of turning depending on cultivation conditions. It will be interesting to uncover neural circuits that underlie plasticity in the ASER-dependent turning initiation and identify neurons controlled by ASG in the neural circuits. ASG is further activated when turning is initiated and contributes to improving accuracy of the salt avoidance behavior (Fig. 8 *B*, *Right*). Again, this is probably achieved by increasing the gain of functional connection between ASER (detection of $dC/dt < 0$) and initiation of sharp turns.

Previous studies have identified and described the pirouette mechanism used in chemotaxis, thermotaxis, and aerotaxis. In this strategy, dependency of the probability of pirouette on temporal changes in sensory input determines the overall migration bias. Also, the relationship between initial and final bearing in each pirouette was studied previously for salt chemotaxis and nonrandom choice of ΔB was noted (16). However, it was not further examined in subsequent studies, and the concept of the pirouette mechanism usually does not include "directed pirouette." A conceptually similar mechanism was recently proposed for odor avoidance behavior (33). In this case, at the end of pirouette worms choose the direction away from the aversive odor source, although precise behavioral components to achieve this have not been determined (33). The reorientation during pirouette is more efficient than weathervane behavior during run (Fig. 7), and ASG, which is activated upon reversal (Fig. 5), likely acts to enhance the reorientation behavior after the first reversal during pirouette.

As in other organisms, neurotransmission in *C. elegans* utilizes classical neuromodulators, including monoamines as well as neuropeptides. In addition to the possibility of regulation through synaptic output of ASG neurons discussed above, there is also a possibility that the neuromodulators expressed in ASG lead to the behavioral transition in taste avoidance learning. According to recent reports, tyramine secreted from RIM neurons controls the omega turn by inhibiting GABAergic RME motor neurons via SER-2 signaling (34, 35). It is necessary to investigate whether ASG is directly related to the head-bending circuit, which is likely important for the directionality during turns. Serotonin modulates various stress responses and behavioral changes. Serotonin levels were increased in ASG sensory neurons by hypoxic stress and the overproduced serotonin enhanced chemotaxis to salt (36). On the other hand, ASG neurons are also known to express FMRF amide-related neuropeptides in addition to serotonin and glutamate. We therefore tested salt chemotaxis of mutants of FMRF amide-related neuropeptides, *flp-6* (JN1673), *flp-13* (JN1664), and *flp-22* (JN2130), but these mutants did not show any abnormalities in taste avoidance learning (*SI Appendix*, Fig. S8). There still remains a possibility that the neurotransmitters other than these FLP peptides are involved in taste avoidance learning. In conclusion, our results suggested that ASER and ASG sensory neurons, the latter's role in taste avoidance learning having been previously unknown, work together to sense both salt concentration and the presence or absence of food and then direct locomotion to efficiently avoid undesired salt concentrations based on previous experience.

Materials and Methods

Strains and Culture. Bristol N2 animals were used as a wild-type strain of *C. elegans*. Worms were cultivated on standard nematode growth medium (NGM) plates using standard methods (37). *Escherichia coli* strain OP50 was fed to animals under normal cultivation conditions and to animals used for calcium imaging, and *E. coli* strain NA22 was fed to animals used for behavioral assays. *C. elegans* strains used in this study are listed in *SI Appendix*, Table S1. The *dyf-11*(*pe554*) background strains used for behavioral assays were grown to adults for 5 d. Other strains, including N2, were grown for 4 d at 20 °C. Transgenic strains were generated by microinjection of transgene DNA (38) or by genetic crosses (37). For detailed information on behavioral assay and analysis, optogenetic stimulation, Ca^{2+} imaging, molecular biology, and statistics, see *SI Appendix, SI Materials and Methods*.

ACKNOWLEDGMENTS. We thank the Caenorhabditis Genetics Center and the laboratory of Cornelia I. Bargmann for providing strains and plasmids that contained histamine-gated chloride channel (HisCl1). We also thank members of the Y.I. laboratory for helpful comments and advice with the experiments. This work was supported by the Core Research for Evolutional Science and Technology program (CREST) "Creation of Fundamental Technologies for Understanding and Control of Biosystem Dynamics," Grant JPMJCR12W1, of the Japan Science and Technology Agency; Japan Society for the Promotion of Science KAKENHI Grant-in-Aid for Scientific Research (S) Grant JP17H06113; and the University of Tokyo Center for Integrative Science of Human Behavior (CiSHuB).

1. C. I. Bargmann, H. R. Horvitz, Chemosensory neurons with overlapping functions direct chemotaxis to multiple chemicals in *C. elegans*. *Neuron* **7**, 729–742 (1991).
2. S. Saeki, M. Yamamoto, Y. Iino, Plasticity of chemotaxis revealed by paired presentation of a chemoattractant and starvation in the nematode *Caenorhabditis elegans*. *J. Exp. Biol.* **204**, 1757–1764 (2001).
3. E. M. Hedgecock, R. L. Russell, Normal and mutant thermotaxis in the nematode *Caenorhabditis elegans*. *Proc. Natl. Acad. Sci. U.S.A.* **72**, 4061–4065 (1975).
4. H. A. Colbert, C. I. Bargmann, Odorant-specific adaptation pathways generate olfactory plasticity in *C. elegans*. *Neuron* **14**, 803–812 (1995).
5. S. R. Wicks, C. H. Rankin, Integration of mechanosensory stimuli in *Caenorhabditis elegans*. *J. Neurosci.* **15**, 2434–2444 (1995).
6. J. G. White, E. Southgate, J. N. Thomson, S. Brenner, The structure of the nervous system of the nematode Caenorhabditis elegans. *Philos. Trans. R. Soc. Lond. B Biol. Sci.* **314**, 1–340 (1986).
7. H. Kunitomo *et al*., Concentration memory-dependent synaptic plasticity of a taste circuit regulates salt concentration chemotaxis in *Caenorhabditis elegans*. *Nat. Commun.* **4**, 2210 (2013).
8. L. Luo *et al*., Dynamic encoding of perception, memory, and movement in a *C. elegans* chemotaxis circuit. *Neuron* **82**, 1115–1128 (2014).
9. M. Tomioka *et al*., The insulin/PI 3-kinase pathway regulates salt chemotaxis learning in *Caenorhabditis elegans*. *Neuron* **51**, 613–625 (2006).
10. S. Oda, M. Tomioka, Y. Iino, Neuronal plasticity regulated by the insulin-like signaling pathway underlies salt chemotaxis learning in *Caenorhabditis elegans*. *J. Neurophysiol.* **106**, 301–308 (2011).
11. T. Adachi *et al*., Reversal of salt preference is directed by the insulin/PI3K and Gq/PKC signaling in *Caenorhabditis elegans*. *Genetics* **186**, 1309–1319 (2010).
12. R. K. Hukema, S. Rademakers, M. P. Dekkers, J. Burghoorn, G. Jansen, Antagonistic sensory cues generate gustatory plasticity in *Caenorhabditis elegans*. *EMBO J.* **25**, 312–322 (2006).
13. T. R. Thiele, S. Faumont, S. R. Lockery, The neural network for chemotaxis to tastants in Caenorhabditis elegans is specialized for temporal differentiation. *J. Neurosci.* **29**, 11904–11911 (2009).
14. T. Murayama, J. Takayama, M. Fujiwara, I. N. Maruyama, Environmental alkalinity sensing mediated by the transmembrane guanylyl cyclase GCY-14 in C. elegans. *Curr. Biol.* **23**, 1007–1012 (2013).
15. A. Zaslaver *et al*., Hierarchical sparse coding in the sensory system of *Caenorhabditis elegans*. *Proc. Natl. Acad. Sci. U.S.A.* **112**, 1185–1189 (2015).
16. J. T. Pierce-Shimomura, T. M. Morse, S. R. Lockery, The fundamental role of pirouettes in *Caenorhabditis elegans* chemotaxis. *J. Neurosci.* **19**, 9557–9569 (1999).
17. Y. Iino, K. Yoshida, Parallel use of two behavioral mechanisms for chemotaxis in *Caenorhabditis elegans*. *J. Neurosci.* **29**, 5370–5380 (2009).
18. Y. Satoh *et al*., Regulation of experience-dependent bidirectional chemotaxis by a neural circuit switch in *Caenorhabditis elegans*. *J. Neurosci.* **34**, 15631–15637 (2014).
19. H. Kunitomo, Y. Iino, *Caenorhabditis elegans* DYF-11, an orthologue of mammalian Traf3ip1/MIP-T3, is required for sensory cilia formation. *Genes Cells* **13**, 13–25 (2008).
20. K. Yoshida *et al*., Odour concentration-dependent olfactory preference change in *C. elegans*. *Nat. Commun.* **3**, 739 (2012).
21. E. A. Pnevmatikakis *et al*., Simultaneous denoising, deconvolution, and demixing of calcium imaging data. *Neuron* **89**, 285–299 (2016).
22. S. Sankaranarayanan, D. De Angelis, J. E. Rothman, T. A. Ryan, The use of pHluorins for optical measurements of presynaptic activity. *Biophys. J.* **79**, 2199–2208 (2000).
23. P. Laurent *et al*., Genetic dissection of neuropeptide cell biology at high and low activity in a defined sensory neuron. *Proc. Natl. Acad. Sci. U.S.A.* **115**, E6890–E6899 (2018).
24. R. van de Bospoort *et al*., Munc13 controls the location and efficiency of dense-core vesicle release in neurons. *J. Cell Biol.* **199**, 883–891 (2012).
25. J. M. Gray, J. J. Hill, C. I. Bargmann, A circuit for navigation in *Caenorhabditis elegans*. *Proc. Natl. Acad. Sci. U.S.A.* **102**, 3184–3191 (2005).
26. J. G. Culotti, R. L. Russell, Osmotic avoidance defective mutants of the nematode *Caenorhabditis elegans*. *Genetics* **90**, 243–256 (1978).
27. P. Sengupta, J. H. Chou, C. I. Bargmann, odr-10 encodes a seven transmembrane domain olfactory receptor required for responses to the odorant diacetyl. *Cell* **84**, 899–909 (1996).
28. A. Solomon *et al*., *Caenorhabditis elegans* OSR-1 regulates behavioral and physiological responses to hyperosmotic environments. *Genetics* **167**, 161–170 (2004).
29. Y. Zhang, H. Lu, C. I. Bargmann, Pathogenic bacteria induce aversive olfactory learning in Caenorhabditis elegans. *Nature* **438**, 179–184 (2005).
30. S. H. Chalasani *et al*., Dissecting a circuit for olfactory behaviour in *Caenorhabditis elegans*. *Nature* **450**, 63–70 (2007).
31. A. J. Chang, N. Chronis, D. S. Karow, M. A. Marletta, C. I. Bargmann, A distributed chemosensory circuit for oxygen preference in *C. elegans*. *PLoS Biol.* **4**, e274 (2006).
32. H. Ohno *et al*., Role of synaptic phosphatidylinositol 3-kinase in a behavioral learning response in *C. elegans*. *Science* **345**, 313–317 (2014).
33. Y. Tanimoto *et al*., Calcium dynamics regulating the timing of decision-making in *C. elegans*. *eLife* **6**, e21629 (2017).
34. J. L. Donnelly *et al*., Monoaminergic orchestration of motor programs in a complex *C. elegans* behavior. *PLoS Biol.* **11**, e1001529 (2013).
35. Y. Kagawa-Nagamura, K. Gengyo-Ando, M. Ohkura, J. Nakai, Role of tyramine in calcium dynamics of GABAergic neurons and escape behavior in *Caenorhabditis elegans*. *Zoological Lett.* **4**, 19 (2018).
36. R. Pocock, O. Hobert, Hypoxia activates a latent circuit for processing gustatory information in *C. elegans*. *Nat. Neurosci.* **13**, 610–614 (2010).
37. S. Brenner, The genetics of Caenorhabditis elegans. *Genetics* **77**, 71–94 (1974).
38. C. C. Mello, J. M. Kramer, D. Stinchcomb, V. Ambros, Efficient gene transfer in *C.elegans*: Extrachromosomal maintenance and integration of transforming sequences. *EMBO J.* **10**, 3959–3970 (1991).